Dynamic and wide field domain observation of amorphous ribbons with longitudinal Kerr effect microscopy

M. Takezawa,[a)] K. Kitajima, Y. Morimoto, and J. Yamasaki

Department of Applied Science for Integrated System Engineering, Kyushu Institute of Technology,
1-1 Sensui-cho, Tobata-ku, Kitakyushu, Fukuoka 804-8550, Japan

Wide field and dynamic domain observation has been done to investigate re-entrant characteristics of amorphous ribbons by adjusting a light path of a Kerr microscope and by triggering a CCD camera. It has been shown that a wide field of 2.6 mm × 2.3 mm with less image distortion was achieved by critical modulation of the light path between an objective lens and samples. The remagnetization process of amorphous ribbons with pinned walls starts with wall depinning and reverse domain nucleation. © *2005 American Institute of Physics.* [DOI: 10.1063/1.1853205]

I. INTRODUCTION

Wide field domain observation of amorphous metal ribbons is a technical issue on the development of magnetic sensors, such as RFID tags used in the industry for identification using radio techniques, based on wall depinning.[1] An objective lens with low magnification for the wide field observation has a working distance as long as a few 10 mm which is too large to secure the suitable incident angle of polarized light around 45° in a longitudinal Kerr effect microscope. So that, a specimen is tilted in general to keep a reasonable incident light angle and mounted under an objective lens in the conventional low magnification domain observation.[2,3] However, tilting the specimen relative to an objective generates image distortion. To eliminate such an image distortion, effort was made to modulate the light path between samples and objective lens. In the present work, a new Kerr microscope by which a wide field domain observation without image distortion is possible has been proposed at first. Using a new Kerr microscope and triggered CCD camera, dynamic domain observation was performed on amorphous ribbons with pinned walls and their re-entrant characteristics[4–7] were investigated.

II. EXPERIMENT

Figure 1 shows a schematic view of mirrors and prisms put between an objective lens and sample stage of a Kerr microscope. The mirrors and prisms were put symmetrically to keep the incident angle of polarizing light around 45° to obtain domain images with high contrast in low magnification. A schematic of the dynamic domain observation system fabricated in this work is shown in Fig. 2. The system consists of a CCD camera, a delay pulse generator, a function generator, an amplifier, an image integrator, and the Kerr microscope. The CCD camera and an ac field was synchronized with a delay setting observation point to observe the dynamic domain image. The delay pulse generator was used for the synchronization as shown in the timing chart of Fig.
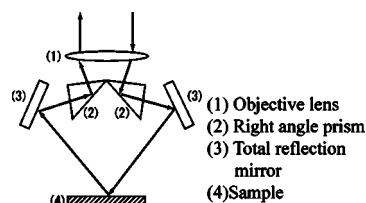

FIG. 1. A schematic view of mirrors and prisms put between the objective lens and sample.

(1) Objective lens
(2) Right angle prism
(3) Total reflection mirror
(4) Sample

3. The shutter speed of the camera triggered through the delay pulse generator is 0.1 ms and the frequency of the trigger pulse and ac field was set 60 Hz being commercial frequency. The 250 frames of the captured periodic domain images were integrated with the image integrator to enhance the contrast.

A nonmagnetostrictive $Fe_{74.26}Co_{4.74}Si_{2.1}B_{18.9}$ amorphous ribbon was observed by the dynamic domain observation system. The dimensions for the thickness, width and length of the ribbon are 22 μm, 2 mm, and 45 mm, respectively. Uniaxial anisotropy along the longitudinal direction was induced by a dc field annealing of 36 kA/m at 280 °C for 30 min, and then the ribbon was annealed for 30 min at 300 °C without the field to have pinned walls caused by the self-induced anisotropy. Applying an ac field at 60 Hz along the longitudinal direction to the ribbon, the dynamic domain observation was done.

III. RESULTS AND DISCUSSION

Figure 4 shows dynamic domain patterns of the nonpinned ribbon in an ac field of ±96 A/m at 60 Hz when the
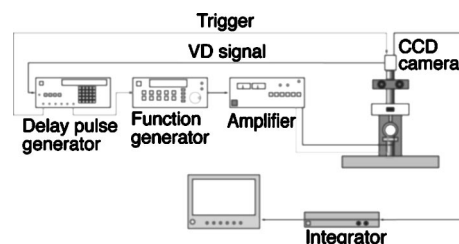

FIG. 2. The system of the dynamic domain observation.

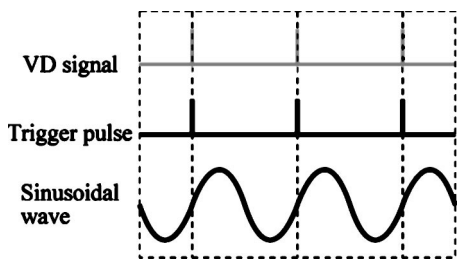a)Author to whom correspondence should be addressed. Electronic mail: take@ele.kyutech.ac.jp

FIG. 3. A timing chart for the dynamic observation.

FIG. 5. A comparison of: (a) a dynamic image with (b) a static domain image.

phase of sinusoidal field is $16\pi/16$ (0 A/m) and $18\pi/16$ (-36.7 A/m), respectively. The field of 96 A/m is enough to saturate the ribbon. The observation area in Fig. 4 is 2.6 mm$\times$2.3 mm. The dark and bright domains have magnetizations pointing in upward and downward directions, respectively. Free walls observed in the figure moved to the center through the distance of 0.3 mm in 1 ms when the field changed from 0 A/m to -36.7 A/m. The speed of the free wall motion is about 0.3 m/s in this case.

Figure 5 shows a comparison of a dynamic domain image with a static domain image. The dynamic image is indistinct at the boundary between dark and bright domains compared to that of the static image because of wall motion during exposure. Nevertheless, the dynamic image observed at the shutter speed of 0.1 ms is clear enough to investigate the magnetization process of amorphous ribbons at 60 Hz. These results indicate that the domain observation in a wide field of 2.6 mm$\times$2.3 mm can be realized and the shutter speed of 0.1 ms allows the dynamic domain observation of amorphous ribbons at 60 Hz.

The dynamic domain patterns of the wall-pinned ribbon at an applied field of ±64 A/m and 60 Hz are shown in Fig. 6. The field of 64 A/m is enough to saturate the ribbon. The magnetization curve in Fig. 6 is the sketch estimated qualitatively by the domain images. The pinned-wall in the left side in Fig. 6(a) kept the position below an applied field of $+24.4$ A/m. When the phase became to $3\pi/16$ ($+35.2$ A/m), the gray contrast between the dark and bright contrast can be seen in Fig. 6(b). If a depinning field has the fluctuations in the required field to depin walls, the contrast at the area of single-shot pictures is dark or bright against each state before or after depinning, respectively. Integration
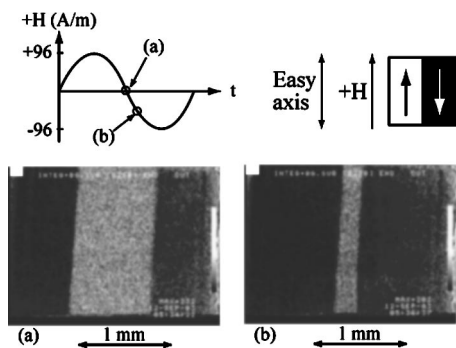
of the periodic pictures results in the gray contrast, which indicates that the amorphous ribbon had the fluctuations of wall depinning field.

Continuous change in the contrast, on the other hand, was observed in the left-hand side in Fig. 6(d) at the phase of $18\pi/16$(-24.8 A/m). The continuous change exhibits wall motion due to nucleation of a reverse domain because the wall displacement of the free wall is different at each cycle of the phase. The results show that the dynamic domain observation made it possible to distinct the magnetization reversal process of the amorphous ribbon between the wall depinning and reverse domain nucleation.

IV. CONCLUSION

In the present work, wide field and dynamic domain observation with mirrors and prisms set under an objective lens and a triggered CCD camera has been performed to investigate the magnetization process of amorphous ribbons. It has been shown that a wide field domain viewing of 2.6 mm $\times$2.3 mm with less image distortion was achieved by critical modulation of the light path between an objective lens and samples, and that re-entrant characteristics of amorphous ribbons with pinned wall was attributable to both wall depinning and reverse domain nucleation. Though higher shutter

FIG. 6. The dynamic domain images: (a) the phase of ac field is $2\pi/16$, (b) $3\pi/16$, (c) $17\pi/16$, (d) $18\pi/16$.

FIG. 4. The dynamic image: (a) the phase of ac field is $16\pi/16$ and (b) $18\pi/16$.

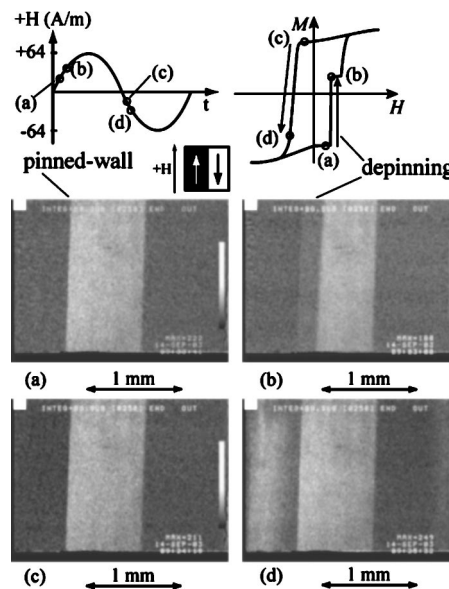speed is required to observe a magnetization process at higher frequencies, the observation technique will allow us to investigate the depinning process of sensor elements such as RFID tags.

[1] J. Yamasaki, K. Mohri, K. Watari, and K. Narita, IEEE Trans. Magn. **20**, 1855 (1984).

[2] E. Feldtkeller and K. U. Stein, Z. Angew. Phys. **23**, 100 (1967).

[3] A. Hubert and R. Schäfer, *Magnetic Domains* (Springer, Germany, 1998), Vol. 27.

[4] J. Yamasaki, M. Takajo, and B. Humphrey, IEEE Trans. Magn. **29**, 2545 (1993).

[5] M. Takajo and J. Yamasaki, J. Magn. Soc. Jpn. **24**, 663 (2000).

[6] J. J. Becker, IEEE Trans. Magn. **9**, 161 (1973).

[7] F. Humphrey, Mater. Sci. Eng., A **179/180**, 66 (1994).